This is an *Accepted Manuscript*, which has been through the Royal Society of Chemistry peer review process and has been accepted for publication.

*Accepted Manuscripts* are published online shortly after acceptance, before technical editing, formatting and proof reading. Using this free service, authors can make their results available to the community, in citable form, before we publish the edited article. We will replace this *Accepted Manuscript* with the edited and formatted *Advance Article* as soon as it is available.

You can find more information about *Accepted Manuscripts* in the Information for Authors.

Please note that technical editing may introduce minor changes to the text and/or graphics, which may alter content. The journal's standard Terms & Conditions and the Ethical guidelines still apply. In no event shall the Royal Society of Chemistry be held responsible for any errors or omissions in this *Accepted Manuscript* or any consequences arising from the use of any information it contains.

# PCCP Guidelines for Referees

***Physical Chemistry Chemical Physics*** (***PCCP***) **is a high quality journal with a large international readership from many communities**

Only very important, insightful and high-quality work should be recommended for publication in *PCCP*.

**To be accepted in *PCCP*** - a manuscript <u>must</u> report:

- Very high quality, reproducible new work

- **Important new physical insights** of significant general interest

- A novel, stand-alone contribution

**Routine or incremental work** should <u>not</u> be recommended for publication. Purely synthetic work is not suitable for PCCP

If you rate the article as 'routine' yet recommend acceptance*,* please give specific reasons in your report.

**Less than 50%** of articles sent for peer review are recommended for publication in *PCCP*. The current PCCP Impact Factor is 3.83

*PCCP* is proud to be a leading journal. We thank you very much for your help in evaluating this manuscript. Your advice as a referee is greatly appreciated.

With our best wishes,

Philip Earis (pccp@rsc.org)                                        Prof Daniella Goldfarb
Managing Editor, PCCP                                             Chair, PCCP Editorial Board

---

**General Guidance (For further details, see the RSC's Refereeing Procedure and Policy)**

Referees have the responsibility to treat the manuscript as confidential. Please be aware of our **Ethical Guidelines** which contain full information on the responsibilities of referees and authors.

*When preparing your report, please:*
• Comment on the originality, importance, impact and scientific reliability of the work;
• State clearly whether you would like to see the paper accepted or rejected and give detailed comments (with references) that will both help the Editor to make a decision on the paper and the authors to improve it;

*Please inform the Editor if:*
• There is a conflict of interest;
• There is a significant part of the work which you cannot referee with confidence;
• If the work, or a significant part of the work, has previously been published, including online publication, or if the work represents part of an unduly fragmented investigation.

*When submitting your report, please:*
• Provide your report rapidly and within the specified deadline, or inform the Editor immediately if you cannot do so. We welcome suggestions of alternative referees.

Dear Editor,

The authors would like to thank the Referee for all suggestions and comments and have revised the manuscript accordingly. In the following, we respond to these comments and describe the corresponding changes in the manuscript:

Referee #1

1.     The fragmentation pattern of 2-thiouracil is very reach, which determines a fairly long discussion. Shortening the results and discussion section would cause a lack of consistency. We do believe that this section is not too long and we prefer to keep it in the present form.

2.     We have defined the term TU as 2-thiouracil.

3.     We have changed the term "ballistic free electrons" for "ballistic electrons".

4.     We have included the energies of the corresponding anion states into Figure 1.

We hope that the manuscript can now be accepted for publications.

Sincerely yours,
Janina Kopyra

Graphical abstract:

Electron induced fragmentation of 2-thiouracil.
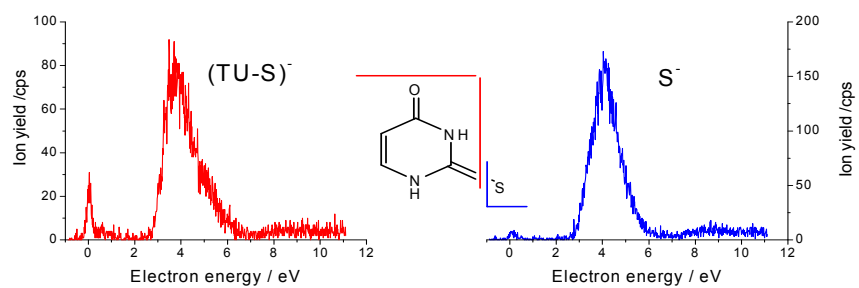
# Electron driven reactions in sulphur containing analogue of uracil: the case of 2-thiouracil

**J. Kopyra[1,*], H. Abdoul-Carime[2], F. Kossoki[3], M.T. do N. Varella[3]**

[1] *Chemistry Department, Siedlce University, 3 Maja 54, 08-110 Siedlce, Poland*

[2] *Université de Lyon, F-69003, Lyon, France; Université Lyon 1, Villeurbanne; CNRS/IN2P3, UMR5822, Institut de Physique Nucléaire de Lyon*

[3] *Instituto de Fisica, Universidade de São Paulo, Caixa Postal 66318, 05314-970 São Paulo, São Paulo, Brazil*

## ABSTRACT

The fragmentation of 2-thiouracil (TU) molecules induced by low energy (< 12 eV) electrons is investigated experimentally and theoretically. It is observed that most of the damage is localised at the sulphur site and in particular visible via the production of the thiocyanate, $SCN^-$, anion. Similarly to the canonical nucleobases the loss of the hydrogen atom is a predominant dissociation channel already at the subexcitation energies. The theory shows that for incident electron energies below 3 eV dissociative electron attachment is initiated by shape resonances implicating the $\pi^*$ molecular orbitals. It may also arise from dipole bound supported state as illustrated by the production of the $SCN^-$, $S^-$ and $(TU - S)^-$ fragments observed close to 0 eV but also the formation of $(TU - H)^-$ species at 0.7 and 1 eV.

---

* corresponding author: kopyra@uph.edu.pl

1

## INTRODUCTION

The interactions of low energy electrons with molecules of biological interest have attracted a considerable attention in the last decade, since it has been demonstrated the ability of these species to damage DNA [1]. These particles (i) are copiously produced along the ionization tracks [2], (ii) have an energy distribution below 15 eV [3] and finally (iii) at these energies the molecular dissociation occurs, in general, with large cross sections [4,5,6]. Paradoxically these geno-toxic effects are highly desirable for therapies that combine the use of radiation and chemical agents with sensitizing properties. Halouracils have been one of the first potential radiosensitizers suggested in the early sixties [7]. One proposed mechanism involves thermalised or pre-hydrated electrons that cause the dissociation of the halo-substituted nucleobases leading to production of the reactive uracil-yl radicals which then become precursors for DNA damage [8]. In fact it has been demonstrated that this mechanism involves rather ballistic electrons [9,10,11]. Further to the studies the results from DFT calculations [12] for a series of uracil derivatives suggest that in particular C5 site is convenient for the implementation of a sensitizing substituent since it is easily modified chemically [13] and not involved in hydrogen bonding between complementary nucleobases within DNA. More recent results obtained for various fluoro-substituted nucleosides show that the sensitization can be achieved not only by the implementation of the halogen atom at the base site but also at the sugar site [14].

Thiolated nucleobases are well known as anti-cancer drugs [15]. Within the last years these molecules also attracted attention in synthetic biology [16] that contributes to improve health care, for instance towards immunodeficiency viruses [17]. The combined use of such analogues of nucleobases and light has been shown to develop sensitization properties [18]. However, these may also induce unwanted and dramatic secondary effects such as skin cancers [19]. Therefore it is desirable to understand how the sulphur-substituted nucleobases can be altered by the ballistic secondary electrons.

In this work, we present the fragmentation of 2-thiouracil (TU) induced by low energy electrons. The most favored dissociation channel produces the (TU - H)⁻ negative ion followed by the formation of the SCN⁻ anion. The sulphur containing site remains nevertheless weak towards low energy electron attacks. The description of the formation of the transient negative ion by the capture of the excess electron is discussed. In order to evaluate the anion spectra of TU we computed elastic integral cross sections, by means of the Schwinger Multichannel Method with Pseudopotentials. The only available theoretical results on the anion states of TU was reported by Dolgounitcheva *et al*. [20]. Their calculations

2

indicate a negative vertical electron attachment energy, that is, the lowest-lying anion would be unstable relative to autodetachment and would be regarded as a resonance.

## EXPERIMENTAL PROCEDURE

We have performed electron/thiouracil collision experiments in a crossed-beam arrangement consisting of an electron source, an oven and a quadrupole mass analyzer (QMA). The components are housed in a UHV chamber at a base pressure of approximately $3\times10^{-9}$ mbar. A well-defined electron beam generated from a trochoidal electron monochromator (resolution ≈250 meV FWHM), orthogonally intersects with an effusive molecular beam of thiouracil. This latter emanates from the vessel (containing approximately 1 mg of ≥98 % purity powder (Alfa Aesar)) heated by two *in vaccuo* halogen bulbs. These lamps also prevent the powder from condensation on the surfaces. In the present work, the material is heated up to 420 K, measured by a platinum resistance. This temperature is however well below the melting temperature (≈ 613 K [21]). Furthermore IR and UV spectroscopic measurements of the vapor substance undertaken at 500 K , do not indicate any decomposition of the products [22]. Since our working temperature is well below 500 K the presently evaporated molecules are likely to remain intact. Upon heating, the molecule may adopt different tautomeric forms [22]. However, from the spectroscopy experiments, only the keto tautomer for which the structure is exhibited in Figure 1 has been reported [22]. Negative ions that are produced in reaction zone after collision of intact molecules with electrons are extracted from the interaction area by a small draw-out-field ($<$ 1 Vcm$^{-1}$), analyzed by the QMA and detected by single pulse counting techniques. The electron energy scale is calibrated by using the $SF_6$ gas flowing through the oven yielding the well-known $SF_6^-$ resonance near zero eV. However, the measurements are performed without the presence of the calibration gas avoiding unwanted reactions such as dissociative electron transfer with the investigated molecules producing an additional signal near 0 eV [23].

## COMPUTATIONAL METHODS

The scattering calculations were performed at the ground state equilibrium geometry. Geometry optimization was performed at the Moller-Plesset second-order perturbation theory (MP2) with the DZP++G(2d,1p) basis set. The electronic ground state was described at the restricted Hartree-Fock level, employing the set of Cartesian Gaussian basis set generated by Bettega *et al.* [24]. A $5s5p2d$ basis set was employed for the heavier atoms, whose exponents

3

are shown in Table 1, while the 3*s* basis of Dunning **[25]** was employed for the hydrogen atoms. The norm-conserving pseudopotentials of Bachelet, Hamann and Schluter (BHS) **[26]** were used to replace the nuclei and the core electrons of the heavier atoms, in both bound state and scattering calculations. The GAMESS package **[27]** was employed for all the above mentioned electronic structure calculations.

The parallel version **[28]** of the Schwinger multichannel method **[29]** implemented with the BHS pseudopotentials (SMCPP method) **[30]** was employed to compute the elastic cross sections. Details on the method can be found elsewhere so here we only outline the relevant aspects to the present calculations. The working expression for the scattering amplitude is given by

$$f(\vec{k}_f, \vec{k}_i) = -\frac{1}{2\pi} \sum_{m,n} \left\langle S_{\vec{k}_f} \left| V \right| \chi_m \right\rangle (d^{-1})_{m,n} \left\langle \chi_n \left| V \right| S_{k_i} \right\rangle$$

where

$$d_{m,n} = \left\langle \chi_m \left| A^{(+)} \right| \chi_n \right\rangle$$

and

$$A^{(+)} = \frac{\hat{H}}{N+1} - \frac{(\hat{H}P + P\hat{H})}{2} + \frac{VP + PV}{2} - VG_P^{(+)}V$$

In the above equations $\left| S_k \right\rangle$ is an eigenstate of the unperturbed Hamiltonian, $H_0$, given by the product of a plane wave with momentum $\vec{k}$ and the target ground state; $V$ is the interaction potential between the target molecule and the incoming electron; $\hat{H} = E - H$ is the collision energy minus the full Hamiltonian, $H = H_0 + V$; $N$ is the number of electrons in the target; $P$ is a projection operator onto the open electronic states of the target; and $G_P^{(+)}$ is the free particle Green's function projected on the $P$ space.

The scattering wave function is expanded in a basis comprising spin-adapted $(N + 1)$-electron Slater determinants, i.e., configuration state functions (CSF's). These configurations are given by products of target states and single-particle functions (scattering orbitals). In the static-exchange (SE) approximation, the CSFs are generated as $\left| \chi_j \right\rangle = A\left[ \left| \Phi_0 \right\rangle \otimes \left| \varphi_j \right\rangle \right]$, where $A$ is the antisymmetrizer, $\left| \Phi_0 \right\rangle$ is the target ground state, and $\left| \varphi_j \right\rangle$ is the scattering orbital. In the static-exchange plus polarization (SEP) approximation, the CSF space is augmented by configurations generated as $\left| \chi_{ij} \right\rangle = A\left[ \left| \Phi_i \right\rangle \otimes \left| \varphi_j \right\rangle \right]$, where $\left| \Phi_i \right\rangle$ represents a virtual excited

4

target state obtained by promoting a single electron from an occupied (hole) to an unoccupied (particle) orbital. Particle and scattering orbitals were represented by modified virtual orbitals (MVOs) [31] generated from the cationic Fock operator with charge +6. The target molecule belongs to the $C_s$ point group, such that the integral cross section could be decomposed into $A'$ and $A''$ components. For both symmetries, the CSF space was generated by the energy criterion [32] $\varepsilon_{scat} + \varepsilon_{part} - \varepsilon_{hole} < \Delta$, where $\varepsilon_{scat}$, $\varepsilon_{part}$ and $\varepsilon_{hole}$ are the energies of the scattering, particle and hole orbitals, respectively, and $\Delta$ is the energy cut-off ($\Delta$ = -1.05 Hartree in the present calculations), allowing for singlet- and triplet-coupled excitations, resulting in a total of 18,256 configurations (9,235 in the $A'$ symmetry and 9,021 in the $A''$ symmetry).

The present elastic cross sections were not corrected to account for the contribution of the long-range dipole potential to the higher partial waves, since we are mainly interested in obtaining the shape resonance spectra. The dipole contribution would increase the magnitude of the background cross sections arising from higher partial waves, but is not expected to significantly impact the positions and widths of the shape resonances, having signatures in lower angular momentum components. To assign the positions and width of the calculated resonances we performed least-squares fits of the eigenphase sums to a model combining Breit-Wigner profiles (to account for the resonant component) and second degree polynomials (background component).

Figure 1 shows the structure of TU along with virtual molecular orbitals, which will be discussed in connection with the resonance spectrum, namely the three lowest lying unoccupied molecular orbitals (LUMOs) having $\pi^*$ character (LUMO, LUMO+1 and LUMO+6), and the LUMO+5 orbital, with $\sigma^*$ character. They were obtained from restricted Hartree-Fock calculations (6-31(d)G basis set) at the MP2-level optimal geometry  (same basis set), employing the Gamess package [35]. These calculations also allowed for estimates of the vertical attachment energies (VAEs) of the $\pi^*$ anion states, employing the empirical relation [33] given by VAE = 0.64795xVOE - 1.4298, which relates the computed virtual orbital energy VOE and the VAE. The latter can be compared with the resonance energy obtained from scattering calculations and experiment.

A molecular dipole moment greater than 2.5 D is strong enough to support a dipole-bound anion, wherein the extra electron is weakly bound to the positive end of the molecule [34]. The description of dipole states requires very diffuse basis functions, which are not contemplated in the standard Dunning's or Pople's family of diffuse functions. In order to characterize this dipole-bound state, we performed electronic structure calculations with the

5

Gaussian09 **[35]** package and the procedure of Skurski *et al.* **[36]** for generating very diffuse functions, briefly described as follows. The aug-cc-pVDZ basis set was augmented with a set of $6s6p$ diffuse functions placed on the hydrogen atom at the C6 site, which lies on the positive pole of the electric dipole moment. The first exponent in the additional set was obtained by dividing the most diffuse hydrogen exponent in the aug-cc-pVDZ valence set by 4. The subsequent exponents were chosen in an even-tempered fashion, successively dividing each exponent by 4. We applied this procedure for both the *s-* and *p*-type extra functions, such that the most diffuse exponent were $7.261 \times 10^{-6}$ a.u. (*s*-type) and $3.4424 \times 10^{-5}$ a.u. (*p*-type). The singly occupied molecular orbital obtained from an unrestricted Hartree-Fock calculation for the anion employing the diffuse basis set is also shown in Figure 1.

Finally, electron affinity estimates were computed from MP2 calculations for both the neutral and the anion molecules. We also computed the dissociation thresholds for the hydrogen elimination reaction from the N1 and N3 sites. We employed the Gaussian-2 method with MP2 corrections G2(MP2) [**37**], and obtained 0.55 eV (N1 site) and 1.00 eV (N3 site). The harmonic frequencies of the neutral TU molecule were computed with density functional theory (DFT) employing the hybrid B3LYP functional and the aug-cc-pVTZ basis set. We mention in passing that dissociation thresholds obtained with the DFT/B3LYP/aug-cc-pVTZ method are in excellent agreement with the G2(MP2) estimates. Both the DFT and G2(MP2) calculations were carried out with the GAUSSIAN 09 package.

## RESULTS and DISCUSSION

The impact of low-energy (< 12 eV) electrons on 2-thiouracil (128 amu, for the molecular structure see Figure 1) leads to the formation of various anionic fragments detected at m/z 127, 96, 85, 75, 67, 58, 42, 32 and 26. Three of them, namely m/z 127, 96 and 32 that have been ascribed to the (TU - H)⁻, (M - S)⁻ and S⁻ anions, arise from a direct single/double bond rupture. The other species require more complex reactions and their formation proceeds via a multiple bond cleavages. They are attributed by stoichiometry to the (TU - OCNH)⁻ (m/z 85), (TU - $C_3HO$)⁻ (m/z 75), (TU - SCNH - $H_2$)⁻ (m/z 67), SCN⁻ (m/z 58), OCN⁻ (m/z 42) and CN⁻ (m/z 26) anions. The ion yield functions are displayed in Figures 2-4.

The change in the ion yields with respect to the incident electron energy exhibit structures reminiscent of resonant processes. At the investigated energy range (< 12 eV), it is well established that dissociative electron attachment is the resonant mechanism responsible for molecular fragmentation [**38**]. In brief, the incoming electron is captured within the Franck-Condon region of the neutral molecule to form a transient negative ion (TNI). The

6

latter then undergoes dissociation into a negatively charged species and at least one stable neutral radical counterpart. However, the molecular dissociation requires (i) a positive value of the electron affinity of the fragment at which the excess charge is localised and (ii) the dissociation time to be sufficiently short in respect to the electron detachment time. Alternatively the excess electron auto-detaches possibly leaving the molecule in an excited state. Thus the first requirement concerns the existence of the states that can give rise to the negatively charged parent, the second is energy controlled and the third dynamics controlled.

Typically at energies above 3-4 eV the first electronically excited states have been reported for canonical nucleobases [39]. Thus the capture of the excess electrons within this energy range may arise from the core excited resonances (two particle-one hole resonances) [38]. Within the yield function of the $(TU - S)^-$, $SCN^-$ and $S^-$ anions a resonance near 3.7 eV can be observed either as a main peak ($(TU - S)^-$, $SCN^-$), or more or less pronounced shoulder ($S^-$). This feature can be compared to that observed in DEA to $CS_2$, which has been associated to the $^2\Pi_U$ state [40,41]. It is noteworthy that this core-excited resonance can couple to a shape resonance as will be discussed below. The resonance located at 4.1 eV and a shoulder at around 5.1 eV also resemble those observed in the DEA to $CS_2$ experiments. For the triatomic molecule, these resonances have been assigned as core-excited Feshbach resonances. Such anion states consist of two electrons in Rydberg excited states that are bound to a positive ion core, *i.e.,* the grand-parent model [42]. For various molecules, it has been observed that such Rydberg anionic states lie typically 4 eV below that of their corresponding positive ions. For the 2-thiouracil the ionization potential has been determined to be about 12 eV [43]. Thus the structures may be related to such a capture process.

In the energy range below the electronically excited states of the molecules, the observed features are attributed to one-particle shape resonances, which are due to a direct accommodation of the excess electron into unoccupied $\pi^*$ molecular orbital (MO). In Figure 5 we show the contribution from *A'* and *A''* symmetries to the calculated elastic integral cross section, obtained in both the SE and SEP approximations. In the SE calculation, we found three $\pi^*$ shape resonances, hereafter called $\pi_1^*$, $\pi_2^*$ and $\pi_3^*$, located at 1.60, 2.39 and 7.5 eV, respectively. These anion states are associated with electron capture into low-lying unoccupied orbitals with $\pi^*$ character (shown in Figure 1). When correlation-polarisation effects are accounted for, the resonances shift to lower energies and become narrower. The lowest lying $\pi_1^*$ state turned out to be bound by 0.22 eV, as obtained by the diagonalisation of the scattering Hamiltonian in the CSF basis, while the resonant $\pi_2^*$ and $\pi_3^*$ states appear at

7

0.56 and 4.9 eV, respectively. Substitution of oxygen by sulphur at the C2 position in uracil gives rise to 2-thiouracil, and this substitution alters the $\pi^*$ resonance energies. In uracil, our recent SMC calculation **[44]** places the $\pi^*$ resonances at 0.14, 1.76 and 4.83 eV. The substitution has its major effect on the $\pi_2^*$ resonance, which is stabilized by approximately 1.2 eV. The $\pi_1^*$ state is stabilized by about 0.4 eV, changing its character from a resonance in uracil to a bound state in TU. This shift to lower energies is ascribed to the greater electron affinity of sulphur, when compared to oxygen, and has also been observed in other systems **[45,46,47]**. The $\pi_2^*$ resonance is the most affected one, due to the more significant influence of sulphur-centered functions in the corresponding resonant orbital, as seen in Figure 1. As for the high-lying $\pi_3^*$ resonance, only a minor shift to higher energies is observed upon chalcogen substitution, which is expected given the low probability of the corresponding orbital at the sulphur site. The $\pi_3^*$ resonance has a mixed shape and core-excited character, as already discussed for similar molecules **[48,49]**. A larger discrepancy in its energy is expected, since our calculations did not include the neutral excited states in the open-channel space, which would give rise to a core-excited contribution to this resonance. Based on recent comparisons of computed and experimental resonance energies **[43,50,51]**, the $\pi_3^*$ state should be located ~1 eV below our computed value, *i.e.*, around 4 eV.

Employing the empirical law described previously, we obtained the VAEs 0.00, 0.48 and 3.68 eV for the $\pi^*$ states, comparable to the scattering results (–0.22, 0.56 and 4.9 eV). The recently reported calculations of Dolgounitcheva *et al.* **[19]** suggest a $\pi_1^*$ resonance located at 0.17 eV, as obtained from the coupled-cluster CCSD(T) method, even though the less sophisticated PMP2 method (spin contamination free MP2) located this anion state around 0.05 eV. The discrepancy between the present results (shallow bound $\pi_1^*$ anion) and those previously reported (low lying $\pi_1^*$ resonance) is not surprising, since obtaining a balanced description of polarisation for the three $\pi^*$ anion states is challenging. SMCPP calculations for other biomolecules usually agree with electron transmission data within $\approx 0.3$ eV, such that we cannot rule out the possibility of a low-lying $\pi_1^*$ shape resonance.

The *A'* symmetry component presents a structure around 9 eV at the SE approximation. At the SEP level, it moves down to 6.3 eV and a very broad structure becomes discernible around 10 eV. These high-lying structures arise from one or more overlapping $\sigma^*$ shape resonances, where the electron is imprisoned in N-H and/or C-H antibonding orbitals. The main feature from the *A'* symmetry, however, is the low-lying peak observed at 3.2 eV, which is evident only in the SEP result. We assign this feature to a $\sigma^*$ shape resonance, with a

significant anti-bonding character at the C=S bond, as depicted in Figure 1. This resonance, with no analog in uracil, is the main difference in the anion spectra arising from the chalcogen substitution.

Besides the valence anion states obtained from the scattering calculations, the bound-state calculation described before supports the existence of a dipole-bound anion, bound by 64 meV. The singly occupied molecular orbital, shown in Figure 1, locates the excess electron in the vicinity of the C6 site. In uracil, the dipole-bound state is formed in a vibrational Feshbach resonance (VFR), which couples to a dissociative $\sigma_{N1H}*$ resonance, giving rise to peaks reflecting the dipole-bound vibrationally excited states $\nu_{NH} = 2$ and $\nu_{NH} = 3$ [51]. The same mechanism can be invoked to explain the DEA spectra reported here for the (TU - H)⁻ fragment. Assuming that the potential energy curve (PEC) of the dipole bound state along the N1-H bond can be obtained from a vertical shift (64 meV) of the neutral molecule PEC, described in the harmonic approximation, we obtained the VFR energies of 0.39 eV ($\nu_{NH} = 1$), 0.84 eV ($\nu_{NH} = 2$) and 1.29 eV ($\nu_{NH} = 3$). In view of the calculated 0.55 eV threshold for hydrogen elimination from the N1 site, the $\nu_{NH} = 1$ VFR would be a closed channel, while the $\nu_{NH} = 2,3$ VFR estimates are in fair agreement with the experimental peaks for the (TU - H)⁻ fragment around 0.7 eV and 1.0 eV (note that inclusion of anharmonic effects would improve the agreement). In view of the high intensity of the 0.7 eV peak, we could also consider the contribution from an indirect mechanism involving the $\pi_2*$ resonance around 0.56 eV. In fact, the $\pi_2*$ virtual orbital in Figure 1 has a significant probability on the N1-H bond that would favor the coupling to the $\sigma*_{N1-H}$ orbital (not shown here), thus supporting the $\pi_2*/ \sigma*_{N1-H}$ indirect mechanism, even though we cannot come to a final conclusion based on the present analysis. The (TU - H)⁻ anion yield observed here close to 0 eV is also observed in 2-thiothymine [52], but is barely visible in uracil. This low-lying peak could be related to the $\pi_1*$ state in TU, even though this symmetry-forbidden process would require a $\pi_1*/ \sigma*_{N1-H}$ coupling.

The strong peak observed around 4 eV for a series of fragments might emerge from the formation of the high-lying $\pi_3*$ mixed-character resonance, which would be located around 4 eV, as discussed above. This anion state may couple to the $\sigma_{CS}*$ resonance (through symmetry-breaking vibrations), possibly giving rise to the S⁻, (M - S)⁻ or even SCN⁻ fragments, though with significant rearrangement in the latter case. In view of the core-excited character, the electron may also autodetach from the $\pi_3*$ resonance, leaving the neutral molecule in a dissociative excited state. The S⁻ and (M - S)⁻ fragments observed near

9

0 eV might also originate from a $\pi_1*/\sigma_{CS}*$ coupling, as suggested from the corresponding virtual orbitals (see Figure 1). Finally, the $SCN^-$ anion signal shows a structure around 0.5 eV, close to the calculated position of the $\pi_2*$ resonance.

As mentioned above, the second requirement for DEA concern the energetics that controls the molecular fragmentation. Thus the appearance energy (AE) of the negatively charged species can be estimated as the difference between the thermochemical value of the bond dissociation energy (BDE) and the electron affinity (EA) of the neutral fragment capturing the excess electron. It is noteworthy that this estimation of the AE is valid for a simple bond dissociation scheme. For more complex fragmentation pattern, some potential barrier has to be overcome thus increasing the AE value. Finally, at elevated temperature, additional vibrational energies might contribute and thus lower the value of AE.

The resonances in the $(TU - H)^-$ ion yield (Figure 2) resemble that recently reported for the dehydrogenated 5-methyl-2-thiouracil anion (2-thiothymine) [52]. Hence this suggest that the presence of the methyl group at C5 position within 2-thiothymine does not influence the dissociation process resulting in the loss of the neutral hydrogen atom. From the previous experiments for canonical nucleobases it has been concluded that the loss of H atom occurs at the N site, while the C–H bonds are not involved in the production of $(M - H)^-$ (where M is the canonical nucleobase) below 3 eV [4]. More specifically from the experiment on 1-methylthymine and 3-methyluracil the H loss from the N1 position has been attributed to the 1 eV resonance, while the loss of H atom from N3 position to the 1.8 eV resonance. The recent calculations performed for uracil by Li *et al.* pointed out thresholds around 0.78 eV (N1 site) and 1.3 eV (N3 site) [53]. Our present theoretical calculations performed for TU indicate the same trend and we have obtained the dissociation thresholds for the hydrogen elimination that is 0.55 eV (N1 site) and 1.00 eV (N3 site).

The second most dominant reaction channel is observed at m/z 58 and attributed to the formation of the $SCN^-$ ion. The fragment is visible via three energy domain namely below 1.5 eV, between 3-5.5 eV and above 7.5 eV (Figure 3). In general it may contain the N atom either from the N1 or from the N3 position. The energy threshold for the appearance of the fragments, as mentioned above, can be estimated as the difference between the bond dissociation energy (D(R–X)) and the electron affinity (EA(SCN) = 3.537 eV [54]) of the neutral fragment on which the excess electron is localised. Hence from the energetic point of view the fragment anion containing N1 may be slightly more favorable since it would require the cleavage of the weaker N1–H bond.

10

The production of the (TU - S)⁻ and S⁻ anions involves a double C=S bond cleavages. As can be seen from Figure 2 the appearance energy for both anions is equal and amount to 2.7 eV. With the value of BDE(C=S) of 4.66 eV [55] and the EA(S) of 2.077 eV [56], AE(S⁻) is estimated to be 2.58 eV that agrees very well with our experimental observations. The value of the estimated AE and its agreement with experimental results suggests that the vibrational energy induced by the thermal heating has no important contribution. Therefore, for the complementary fragmentation channel, *i.e.,* for the (TU - S)⁻ ion production, the EA(TU - S) is likely to be in the same range as electron affinity of the sulphur atom.

The electron affinities of the cyanide compounds, *i.e.,* OCN and CN are much higher (3.609eV and 3.862 eV, respectively) [54] than those of the sulphur containing fragments. However, their production requires multiple bond cleavage and frequently rearrangement within the precursor ion as shown recently for acetamide and some of its derivatives [57]. From the existing typical bond dissociation energies (BDE(C–C) = 3.9 eV [58], BDE(C–N) = 3.7 eV [58] and BDE(N3–H) = 1.0 eV) and the EA(OCN), the threshold for the production of the OCN⁻ ion is estimated to be around 5 eV. The onset for the formation of the cyanate ion is observed at about 3.1 eV (Figure 3). This suggests the reaction proceeds through molecular rearrangement and formation of new bonds and/or generation of new stable molecules as neutral counterparts to supply the necessary energy for the reaction. Here it is worth noting that in recent studies applying DEA, MALDI, and potassium–molecule collision experiments [59] it has been demonstrated that for the N-site methylated pyrimidine derivatives the OCN⁻ ion is formed in a sequential decay reaction with the dehydrogenated closed shell anion as an intermediate product. Although our experiment does not give such information we cannot exclude such a reaction in the case of presently investigated thio-compound. Furthermore, from the electron transfer experiments in potassium collisions with N-site methylated pyrimidines it has been demonstrated that OCN⁻ branching ratios show a remarkable site- and bond-selectivity in this decay channel [59]. However, for the investigated 2-thiouracil there is only one reaction channel possible that results in the formation of OCN⁻ involving nitrogen atom at N3 position (otherwise the oxygen atom at C2 position is replaced by the sulphur atom). Thus we do not observe the resonance in the energy range 6-7.5 eV reported from pristine thymine as well as its methylated forms at N1 and N3 positions while the resonances between 7.5 and 11 eV are substantially diminished [59]. As the OCN⁻ anion, CN⁻ is also visible from the present experiment via a broad resonance between 3-5.5 eV (Figure 3). In this case, however, some intensity also appears below 2 eV. This suggests that the formation of

11

CN⁻ at this low energy domain is most likely associated with the formation of a neutral stable counterpart(s).

Finally, we observe fragments at m/z 85, m/z 75 and m/z 67 (Figure 4) that have been attributed to the (TU - OCNH)⁻, (TU - $C_3HO$)⁻ and (TU - SCNH - $H_2$)⁻ anions, respectively. The (TU - OCNH)⁻ anion is generated from the loss of the isocyanic acid. Such reaction has been recently reported from guanine, however at much lower energy around 1.3 eV **[60]**. This reaction channel is complementary to the OCN⁻ ion formation with additional loss of the H atom. The intensity of these two latter fragments is almost the same thus we suggest that the electron affinity of the (TU - OCNH) is higher than EA(OCN) by the dissociation energy of the N3–H bond (by 1.0 eV, according to our present calculations). In general, all of these three fragments m/z 85, m/z 75 and m/z 67 are likely generated from same TNI since they are visible at the same energy range around 4 eV. In addition for m/z 67 a broad structure between 8 and 10 eV is observable, however with substantially lower intensity.

## CONCLUSIONS

In the present contribution we discuss the fragmentation dynamics of 2-thiouracil caused by the capture of low energy electrons. The main finding is that the presence of the S atom at the C2 position strongly influences the dissociation and hence the dominant fragments are generated from the sulphur site of the molecule resulting in the formation of, *e.g.,* SCN⁻, S⁻ and (TU - S)⁻. These fragmentation channels are mainly visible via the initial formation of the resonances localised at around 4 eV as predicted by our theoretical calculations. These resonances can emerge from the formation of the high-lying resonant $\pi_3$* state of mixed-character that may couple to the $\sigma_{CS}$* state and hence induce the C=S bond rupture or undergo more complex reaction leading to SCN⁻ formation. The only exception is the production of the dehydrogenated parent anion (TU - H)⁻, which is visible via a series of strongly overlapping structures in the energy range below 4 eV. Two of them that appear at 0.7 eV and 1 eV are most likely due to the dipole-bound mediated vibrational Feshbach resonances. We postulate that the main peak at 0.7 eV can also be generated through the so-called indirect mechanism that proceed via an initial localisation of the excess charge at the $\pi_2$* orbital that couple to the dissociative $\sigma_{NH}$* resonance. Further peak that appears at the threshold energy (around 0 eV) may be due to the $\pi_1$* state, while a broad but clear structure at about 3.2 eV may have its origin from an indirect mechanism involving the high-lying $\pi_3$* resonance and/or the $\sigma_{CS}$* resonance.

12

13

**TABLES**

**Table 1**: Exponents of the uncontracted Cartesian Gaussian function (in atomic units).

## FIGURE CAPTION

**Figure 1:** Structures of the 2-thiouracil (upper left), the three lowest-lying $\pi^*$ (bottom) and the $\sigma_{C=S}^*$ (upper middle) virtual orbitals, and the singly occupied of the dipole-bound state (upper right). Corresponding atoms are marked with colors: S – yellow, N – blue, O – red, C – grey, H – white.

**Figure 2:** Ion yield of (a) $(TU-H)^-$ (m/z 127), (b) $(TU-S)^-$ (m/z 96) and (c) $S^-$ (m/z 32) as a function of the incident electron energy.

**Figure 3:** Ion yield of (a) $SCN^-$ (m/z 58), (b) $OCN^-$ (m/z 42) and (c) $CN^-$ (m/z 26) as a function of the incident electron energy.

**Figure 4:** Ion yield of (a) m/z 85, (b) m/z 75 and (c) m/z 67 as a function of the incident electron energy.

**Figure 5:** Symmetry decomposition of the elastic integral cross section for 2-thiouracil, computed at both the SE and the SEP approximations.

15

**Table 1**

| Type | Carbon | Nitrogen | Oxygen | Sulphur |
|------|--------|----------|--------|---------|
| *s* | 12.496280 | 17.567340 | 16.058780 | 7.6490930 |
| *s* | 2.470286 | 3.423615 | 5.920242 | 1.743283 |
| *s* | 0.614028 | 0.884301 | 1.034907 | 0.789128 |
| *s* | 0.184028 | 0.259045 | 0.316843 | 0.302805 |
| *s* | 0.039982 | 0.055708 | 0.065203 | 0.063479 |
| *p* | 5.228869 | 7.050692 | 10.141200 | 7.203417 |
| *p* | 1.592058 | 1.910543 | 2.783023 | 3.134723 |
| *p* | 0.568612 | 0.579261 | 0.841010 | 0.52938 |
| *p* | 0.210326 | 0.165395 | 0.232940 | 0.154155 |
| *p* | 0.072250 | 0.037192 | 0.052211 | 0.035523 |
| *d* | 0.603592 | 0.403039 | 0.756793 | 1.163168 |
| *d* | 0.156753 | 0.091192 | 0.180759 | 0.240526 |

**REFERENCES**

1    B. Boudaïffa, P. Cloutier, D. Hunting, M. A. Huels and L. Sanche, *Science* **287** 1658 (2000).

2    International Commission on Radiation Units and Measurements, ICRU Report 31 (ICRU, Washington, DC, 1979). $5 \times 10^4$ electrons per MeV primary quantum deposited.

3    T. Jahnke, H. Sann, T. Havermeier, K. Kreidi, C. Stuck, M. Meckel, M. Schöffler, N. Neumann, R.Wallauer, S. Voss, A. Czasch, O. Jagutzki, A. Malakzadeh, F. Afaneh, Th. Weber, H. Schmidt-Böcking, R. Dörner, *Nature Phys.* **139** 6 (2010).

4    H. Abdoul-Carime, S. Gohlke, E. Illenberger, *Phys. Rev. Lett.* **92** 168103 (2004).

5    J. Kopyra, C. Koenig-Lehmann and E. Illenberger, *Int. J. Mass Spectrom.* **281** 89 (2009).

6    I. Baccarelli, I. Bald, F.A. Gianturco, E. Illenberger, J. Kopyra, *Physics Reports* **508** 1 (2011).

7    S. Zamenhof, R. De Giovanni, S. Greer, *Nature* **181** 822 (1958).

8    L. Ling and J.F. Ward, *Radiat. Res.* **121** 76 (1990).

9    H. Abdoul-Carime, P.-C. Dugal, L. Sanche, *Radiat. Res.* **153** 23 (2000).

10   H. Abdoul-Carime, M.A. Huels, L. Sanche, E. Illenberger, *J. Am. Chem. Soc.* **123** 5354 (2001).

11   M. Lamsabhi, M. Alcami, O. Mo, W. Bouab, M. Esseffar, J.-L.M. Abboud, M. Yanez, *J. Phys. Chem. A*, **104** 5122 (2000).

12   L. Chomicz, M. Zdrowowicz, F. Kasprzykowski, J. Rak, A. Buonaugurio, Y. Wang, and K.H. Bowen, *J. Phys. Chem. Lett.* **4** 2853 (2013).

13   E.C. Ressner, P. Fraher, M.S. Edelman, M.P. Mertes, *J. Med. Chem.* **19** 194 (1976).

14   J. Kopyra, A. Keller, I. Bald, *RSC Advances* **4** 6825 (2014).

15   G. B. Elion, *Science* **244** 41 (1989).

16   P. Ball, *Nature* **431** 624 (2004).

17   T. Elbeik et al., *J. Clin. Microbiol* **42** 3120 (2004).

18   G. Cui, W.H. Fang, *J. Chem. Phys.* **138** 044315 (2013).

19   N.R. Attard, P. Karran, *Photochem. Photobiol. Sci.* **11** 62 (2012).

20   O. Dolgounitcheva, V.G. Zakrzewski, J.V. Ortiz, *J. Chem. Phys.* **134** 074305 (2011).

21    M. Lamsabhi, M. Alcami, O. Mo, W. Bouab, M. Esseffar, J.-L.M. Abboud, M. Yanez, *J. Phys. Chem. A* **104** 5122 (2000).

22    H. Rostkowska, A. Barski, K. Szczepaniak, M. Szczesniak, W.B. Person, *J. Mol. Struct.* **176** 137 (1988).

23    S. Gohlke, H. Abdoul-Carime , E. Illenberger, *Chem. Phys. Lett.* **380** 595 (2003).

24    M.H.F. Bettega, A.P.P. Natalense, M.A.P. Lima, and L.G. Ferreira, *Int. J. Quantum Chem.* **60** 821 (1996).

25    T. H. Dunning, Jr., *J. Chem. Phys.* **53** 2823 (1970).

26    G. B. Bachelet, D. R. Hamann, and M. Schluter, *Phys. Rev. B* **26** 4199 (1982).

27    M.W. Schmidt, K.K. Baldridge, J.A. Boatz, S.T. Elbert, M.S. Gordon, J.H. Jensen, S. Koseki, N. Matsunaga, K. A. Nguyen, S.J. Su, T.L. Windus, M. Dupuis, J.A. Montgomery, *J. Comput. Chem.* **14** 1347 (1993).

28    J.S. dos Santos, R.F. da Costa, and M.T. do N. Varella, *J. Chem. Phys.* **136** 084307 (2012).

29    K. Takatsuka and V. McKoy, *Phys. Rev. A* **24** 2473 (1981); **30** 1734 (1984).

30    M.H.F. Bettega, L.G. Ferreira, and M.A.P. Lima, *Phys. Rev.* A **47** 1111 (1993).

31    C.W. Bauschlicher, Jr., *J. Chem. Phys.* **72** 880 (1980).

32    F. Kossoski and M.H.F. Bettega, *J. Chem. Phys.* **138** 234311 (2013).

33    S.W. Staley and J.T. Strnad, *J. Chem. Phys.* **98** 116 (1994).

34    C. Desfrançois, H. Abdoul-Carime, N. Khelifa, J.P. Schermann *Phys. Rev. Lett.* **73** 2436 (1994).

35    M.J. Frisch, G.W. Trucks, H.B. Schlegel, G.E. Scuseria, M.A. Robb, J.R. Cheeseman, G. Scalmani, V. Barone, B. Mennucci, G.A. Petersson, H. Nakatsuji, M. Caricato, X. Li, H.P. Hratchian, A.F. Izmaylov, J. Bloino, G. Zheng, J.L. Sonnenberg, M. Hada, M. Ehara, K. Toyota, R. Fukuda, J. Hasegawa, M. Ishida, T. Nakajima, Y. Honda, O. Kitao, H. Nakai, T. Vreven, J. A. Montgomery, Jr., J.E. Peralta, F. Ogliaro, M. Bearpark, J.J. Heyd, E. Brothers, K.N. Kudin, V.N. Staroverov, R. Kobayashi, J. Normand, K. Raghavachari, A. Rendell, J.C. Burant, S.S. Iyengar, J. Tomasi, M. Cossi, N. Rega, J.M. Millam, M. Klene, J.E. Knox, J.B. Cross, V. Bakken, C. Adamo, J. Jaramillo, R. Gomperts, R.E. Stratmann, O. Yazyev, A.J. Austin, R. Cammi, C. Pomelli, J.W. Ochterski, R.L. Martin, K. Morokuma, V.G. Zakrzewski, G.A. Voth, P. Salvador, J.J. Dannenberg, S. Dapprich, A.D. Daniels, Ö. Farkas, J. B. Foresman, J.V. Ortiz, J. Cioslowski, and D.J. Fox, Gaussian, Inc., Wallingford CT, 2009.

36    P. Skurski, M. Gutowski, and J. Simons, *Int. J. Quant. Chem.* **80** 1024 (2000).

37    L.A. Curtiss, K. Raghavachari, and J.A. Pople, *J. Chem. Phys.* **98** 1293 (1993).

38    E. Illenberger and J. Momigny, *Gaseous Molecular Ions. An Introduction to Elementary Processes Induced by Ionization.* Steinkopff Verlag, Darmstadt / Springer-Verlag, New York, 1992.

39    A.V. Crewe, M. Isaacson, D. Johnson, *Nature* **231** 262 (1971).

40    J.-P. Ziesel, G.J. Schulz, J. Milhaud, *J. Chem. Phys.* **62** 1936 (1975).

41    R. Dressler, M. Allan, M. Tronc, *J. Phys. B: At. Mol. Opt. Phys.* **20** 393 (1987).

42    L. Sanche and G. J. Schulz, *Phys. Rev. A* **6** 69 (1972).

43    A.R. Katrizki, M. Szafran, *J. Chem. Soc. Perkin Trans.* **2** 871 (1990).

44    F Kossoski, M. H. F. Bettega, and M. T. do. N. Varella, *J. Chem. Phys.* **140** 024317 (2014).

45    C. Dezarnaud-Dandine, F. Bournel, M. Tronc, D. Jones, and A. Modelli, *J. Phys. B: At., Mol. Opt. Phys.* **31** L497 (1998).

46    A. Modelli and P. Burrow, *J. Phys. Chem. A* **108** 5721 (2004).

47    R. F. da Costa, M. T. do N. Varella, M. A. P. Lima, and M. H. F. Bettega, *J. Chem. Phys.* **138** 194306 (2013).

48    I. Nenner and G. J. Schulz, *J. Chem. Phys.* **62** 1747 (1975).

49    C. Winstead and V. McKoy, *Phys. Rev. Lett.* **98** 113201 (2007).

50    A. S. Barbosa, D. F. Pastega, and M. H. F. Bettega, *Phys. Rev. A* **88** 022705 (2013).

51    A. S. Barbosa and M. H. F. Bettega, *J. Chem. Phys.* **139**214301 (2013).

52    J. Kopyra, S. Freza, H. Abdoul-Carime, M. Marchaj, P. Skurski, *Phys. Chem. Chem. Phys.* **16** 5342 (2014).

53    X. Li, L. Sanche, and M.D. Sevilla, *J. Phys. Chem. B* **108** 5472 (2004).

54    J.C. Rienstra-Kiracofe, G.S. Tschumper, H.F. Schaeffer III, S. Nandi and G.B. Ellison, *Chem. Rev.* **102** 231 (2002).

55    D. L. Hildenbrand, *Chem. Phys. Lett.* **15** 379 (1972).

56    W.C. Lineberger, B.W. Woodward, *Phys. Rev. Lett.* **25** 424 (1970).

57    C. Koenig-Lehmann, J. Kopyra, I. Dabkowska, J. Kocisek and E. Illenberger, *Phys. Chem. Chem. Phys.* **10** 6954 (2008).

58    S.J. Blanksby and G.B. Ellison, *Acc. Chem. Res.* **36** 255 (2003).

59    F. Ferreira da Silva, C. Matias, D. Almeida, G. García, O. Ingólfsson, H. Dögg
      Flosadóttir, B. Ómarsson, S. Ptasinska, B. Puschnigg, P. Scheier, P. Limão-Vieira, S.
      Denifl, *J. Am. Soc. Mass Spectrom.* **24** 1787 (2013).

60    H. Abdoul-Carime, J. Langer, M.A. Huels, and E. Illenberger, *Eur. Phys. J. D* **35** 399
      (2005).

20

$\sigma^*_{CS}$ (3.2 eV)  $\sigma^*_{dip}$ (-0.064 eV)

$\pi^*_1$ (-0.22 eV)  $\pi^*_2$ (0.56 eV)  $\pi^*_3$ (4.9 eV)
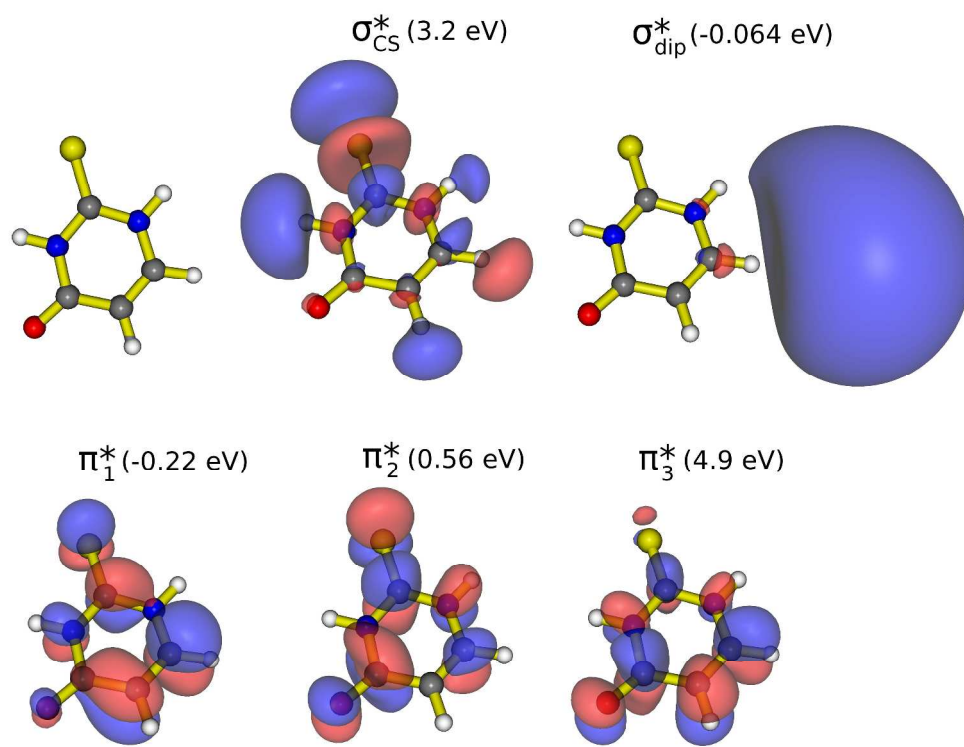
1834x1397mm (100 x 100 DPI)
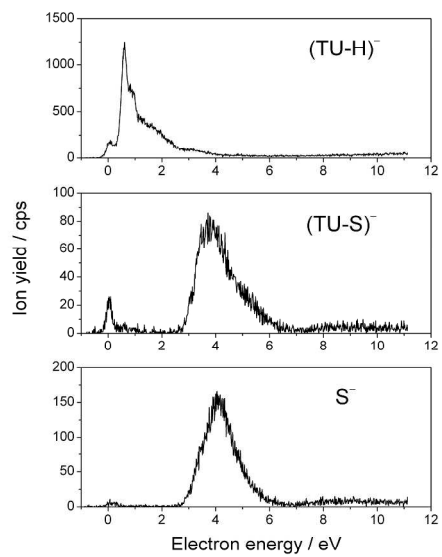
270x189mm (300 x 300 DPI)
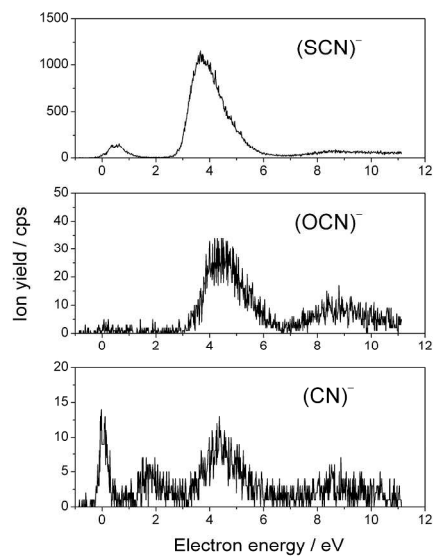
270x189mm (300 x 300 DPI)

156x132mm (100 x 100 DPI)